Food Sci. Biotechnol. Vol. 18, No. 4, pp. 910 ~ 916 (2009)

Food Science and Biotechnology

Influence of Methylcellulose on Properties of Wheat Gliadin Film Cast from Aqueous Ethanol

Yihu Song[1,2]*, Lingfang Li[1], and Qiang Zheng[1,2]

[1]*Department of Polymer Science and Engineering, Zhejiang University, Hangzhou 310027, PR China*

[2]*Key Laboratory of Macromolecular Synthesis and Functionalization of Ministry of Education, Zhejiang University, Hangzhou 310027, PR China*

Abstract Present work was focused on the influence of methylcellulose (MC) on steady rheology of wheat gliadin solution and the properties of glycerol plasticized gliadin films. The presence of MC below 0.99 wt% improved viscosity and flow activation energy of the 10 wt% gliadin solution significantly. In the casting films containing 0.2 g glycerol/g dry protein, the MC component aggregated in the gliadin matrix. The blend films containing less than 7.7 wt% MC exhibited higher Young's modulus (E) and tensile strength (σ_b) and lower elongation at break (ε_b) in comparison with the pure gliadin film, which was related to the intermolecular interaction between MC and gliadins, the brittle fracture of the aggregated MC component, and the increase in glass transition temperature (T_g) of the gliadin phase. Increasing MC content led to a slight increase in water vapor permeability (WVP) without significant influence on the moisture absorption (MA).

Keywords: wheat gliadin, methylcellulose, blend film, mechanical property, morphology

Introduction

Biopolymers from plant/crop based renewable agricultural resources offer alternative options to meet the growing worldwide need for environment-friendly, sustainable materials and to reduce consumption of petroleum and petroleum based plastic package films (1). Wheat proteins have been considered as a class of renewable materials due to its abundant resource, low cost, unique viscoelastic properties, good biodegradability, and excellent barriers to oxygen, carbon dioxide, and some aromatic compounds (2). Gliadins are important storage proteins that provide viscous character to wheat gluten (3,4) and have perfect film forming character (5).

Protein films are usually prepared via solution cast using water and/or ethanol as cosolvent (6). The films without plasticizer are brittle and are difficult to handle thus plasticizer is commonly used to increase chain mobility of proteins (7). Glycerol and ethylene glycols have been used to plasticize gliadins to prepare flexible films (8,9). Glycerol plasticization usually results in marked reduction in stiffness and strength performances (10). Covalent crosslinking of gliadin polypeptide chains using dialdehydes (11) and thermal treatment of the casting films (7) can improve the water vapor barrier and tensile strength properties. Cysteine is also used to mediate the polymerization reaction of gliadins via sulphydryl-disulphide interchange to improve the properties of the resultant films (12).

As the least hydrophilic water-soluble cellulose derivative, methylcellulose (MC) has been used to produce moisture-sensitive films (13) used in pharmaceutical and food industries (14). Polyethylene glycols are effective plasticizers for MC films (13-15). The physical properties of MC films are related to dry temperature, ethanol concentration, plasticizer content, and film thickness (13-18). MC has been combined with fatty acids (19) and polysaccharides (20) to make edible films that can serve as effective barriers to water vapor, oxygen, and carbon dioxide. MC has also been used to blend with whey proteins to prepare films with optimized properties (21,22).

Incorporation of polysaccharides into protein matrices may extend the functional properties of these film-forming ingredients and improve the film performance owing to their variability in physical properties and/or their interactions (21,23). Some polysaccharides can reduce water vapor permeability (WVP) and improve mechanical properties of whey protein films in comparison with the films prepared by polysaccharides and proteins in isolation (21,23,24). Chitosan and cellulose acetate phthalate have been applied to prepare wheat gluten blend films with improved mechanical strength and reduced WVP (25,26). To our knowledge, no investigation regarding the properties of gliadins/MC blend films has been reported to date.

Both gliadins and MC are soluble in aqueous ethanol, making it possible to prepare blend films using the cast method. Protein-polysaccharide mixtures in solutions generally undergo phase separation through thermodynamic incompatibility or complex coacervation depending on the molecular interaction (27). Heat treatment can weaken the low energy bonds responsible for co-solubilization of the protein and polysaccharide, leading to the formation of a continuous protein network with polysaccharide inclusions (28). We in the present study prepared gliadin/MC blend films by casting the gliadin/MC mixture solution and drying at 50°C. Steady rheology of the mixture solutions and the structure and properties of the blend films were investigated for accounting for the effect of MC incorporation.

*Corresponding author: Tel: +86-571-8795-3075; Fax: +86-571-8795-2522
E-mail: s_yh0411@zju.edu.cn
Received December 11, 2008; Revised February 17, 2009;
Accepted February 17, 2009

Materials and Methods

Materials Wheat gluten with a protein content ≥75 wt%, a starch content ≤10 wt%, a fat content ≤6.5 wt%, a cellulose content ≤0.5 wt%, an ash content ≤0.95 wt%, and a moisture content ≤9.0 wt% was supplied by Shanghai Wangwei Food Co., Ltd. (Shanghai, China). Methylcellulose (MC) under the trademark of M450 was purchased from Sinopharm Chemical Reagent Co., Ltd. (Shanghai, China). MC had a moisture content 5 wt%. Glycerol used was of analytical grade.

One-hundred g crude wheat gluten was dispersed in 500 mL 70%(v/v) aqueous ethanol, stirred for 12 hr, and centrifuged at 4,000×g for 15 min at room temperature. The supernatant containing the gliadin-rich fraction was dried at room temperature and was further freeze-dried using a freeze dryer (model FD-1; Beijing Youde Techn. Develop. Co., Ltd., Beijing, China). The dried gliadin-rich fraction was ground to pass through 100 mesh sieve.

Film formation Freeze-dried gliadin powders were dissolved in 70%(v/v) aqueous ethanol to yield a 10 wt% solution. MC of 0, 2.5, 5.0, 7.5, and 10 g/100 g dry protein was added into the solution under stirring until a transparent solution was formed. The MC concentration, C_{MC}, in the gliadin/MC mixture solution was 0, 0.25, 0.50, 0.74, and 0.99 wt%, respectively. The mixture solutions were used for steady viscosity measurement.

Glycerol of 0.2 g/g dry protein was dissolved in the gliadin/MC mixture solution under stirring. The solution of 40 g was poured onto plastic petri dishes with an inner diameter of 90-mm and was dried at 50°C for 3 days. The films were carefully detached and were stored in desiccators at 50% relative humidities (RH) until testing. The weight percentage of MC, w_{MC}, with respect to the total mass of the blend film was 0, 2.0, 4.0, 5.9, and 7.7 wt%, respectively.

Steady viscosity measurement Steady shear measurements were conducted from 1 to 1,000 1/sec to the gliadin/MC mixture solutions using a rotational controlled stress rheometer (model AR-G2; TA Instruments, New Castle, DE, USA) with a 40-mm and 2° cone plate geometry. Three duplicates were measured to obtain mean values of steady viscosity for each solution at 15, 35, and 45°C, respectively. A small amount of 70%(v/v) aqueous ethanol was placed into the solvent trap. The solvent trap cover had a lip that sat in the solvent, allowing the free space around the sample to become saturated with the solvent vapor, which prevented evaporation.

Morphology observation The blend films were stretched to break at room temperature. Morphology of the fracture surface was observed after coating with gold using a scanning electron microscope (SEM) (model SLR10N; FEI, Eindhoven, Netherlands) at 25 kV.

Fourier transformation infrared (FTIR) spectra measurement The solution was coated on potassium bromide plate and was dried under ultraviolet lamp radiation. FTIR spectra were measured using FTIR spectrometer (model VECTOR 22; Bruker Optik. GmbH, Ettlingen, Germany) with a resolution of 4/cm.

Film thickness (H) measurement H was measured using a handheld micrometer (Shanghai Measuring & Cutting Tool Works, Shanghai, China) and was reported as the mean of 9 measurements from different locations of each product.

Tensile mechanical property measurement Tensile test was performed on an universal testing machine (model CMT-4204; Shenzhen SANS Test Machine Co., Ltd., Shenzhen, China) with an extension rate of 10 mm/min at 25°C at 50% RH. The film samples were cut into rectangle shape of 10.0 mm in width and 20.0 mm in length. Young's modulus (E), tensile strength (σ_b), and elongation at break (ε_b) were evaluated from 5 duplicates for each product.

Dynamic mechanical analysis (DMA) DMA was performed at 1 Hz with a dynamic mechanical thermal analyzer (model DMA 242; NETZSCH, Selb, Germany) using tensile mode at a heating rate of 3°C/min. Paraffine oil was coated on the sample surface in order to eliminate moisture interchange between the sample and the surroundings. Storage modulus (E') and loss factor (tan δ) were recorded as a function of temperature T from −100 to 150°C.

Moisture absorption (MA) measurement Triplicate films of 10×50 mm were stored for 1 week until constant weight in an airtight desiccator at 25°C over anhydrous phosphorus pentoxide (P_2O_5). The predried samples were transferred into a desiccator equilibrated at 70% RH and were stored for 72 hr to constant weight. MA was evaluated according to the weight gain over the predried samples and was reported as the mean of 3 replicates.

Water vapor permeability (WVP) measurement WVP of films was determined gravimetrically at 25°C according to ASTM (29) with a slight modification. The predied films were mechanically sealed to glass test cups containing P_2O_5 (0% RH). The exposed area of the test cup was 0.0243 m^2. The cups were placed in an airtight desiccators maintained at 70% RH. WVP was determined after steady-state condition was reached according to $WVP=\Delta wH/A_e\Delta t\Delta p$ (30). Here, Δw is weight gain over time interval Δt, A_e is the area of exposed film and Δp is the vapor pressure across the film.

Water solubility measurement Triplicate predried films of 10×50 mm were immersed in 300 mL deionized water at 25°C for 72 hr with occasional gentle manual agitation. Deionized water was changed twice everyday to avoid microbial growth. The undissolved matter was dried over P_2O_5 at 25°C in the desiccator until constant mass. Weight loss in water (WLW) was calculated according to dry mass before and after immersing (5).

Statistical analyses Statistical analyses were performed using OriginPro 7.50 software (OriginLab Co., Northampton, MA, USA). The data were expressed as the mean value± standard deviation (SD). A one-way analysis of variance (ANOVA) followed by a Tukey test ($p<0.05$) was used to identify whether the differences between the treatments were significant.

Results and Discussion

Rheological behavior of the gliadin/methylcellulose (MC) mixture solutions Influence of C_{MC} on apparent viscosity (η) as a function of shear rate ($\dot{\gamma}$) for the solutions at 15, 35, and 45°C, respectively was shown in Fig. 1. Introduction of MC into the gliadin solution caused a marked increase in η. At $C_{MC} \leq 0.50$ wt%, the solutions approximately behaved as Newtonian liquid because η did not vary with $\dot{\gamma}$ markedly. On the other hand, the solutions at C_{MC}=0.74 and 0.99 wt% exhibited Newtonian, shear thickening and shear thinning behaviors in succession with increasing $\dot{\gamma}$. The hydrogen bonding interaction between MC and gliadins is probably responsible for the origins of the shear thickening and the thinning. The hydrogen bonding interaction interlinks the gliadin macromolecules in the dilute regime, which restricts the molecular orientation along the flow direction and gives rise to the weak shear thickening with increasing $\dot{\gamma}$. On the other hand, the weak shear thinning at high strain rates could be related to the gradual disruption of hydrogen bonding interaction along the aligned gliadin and MC macromolecules.

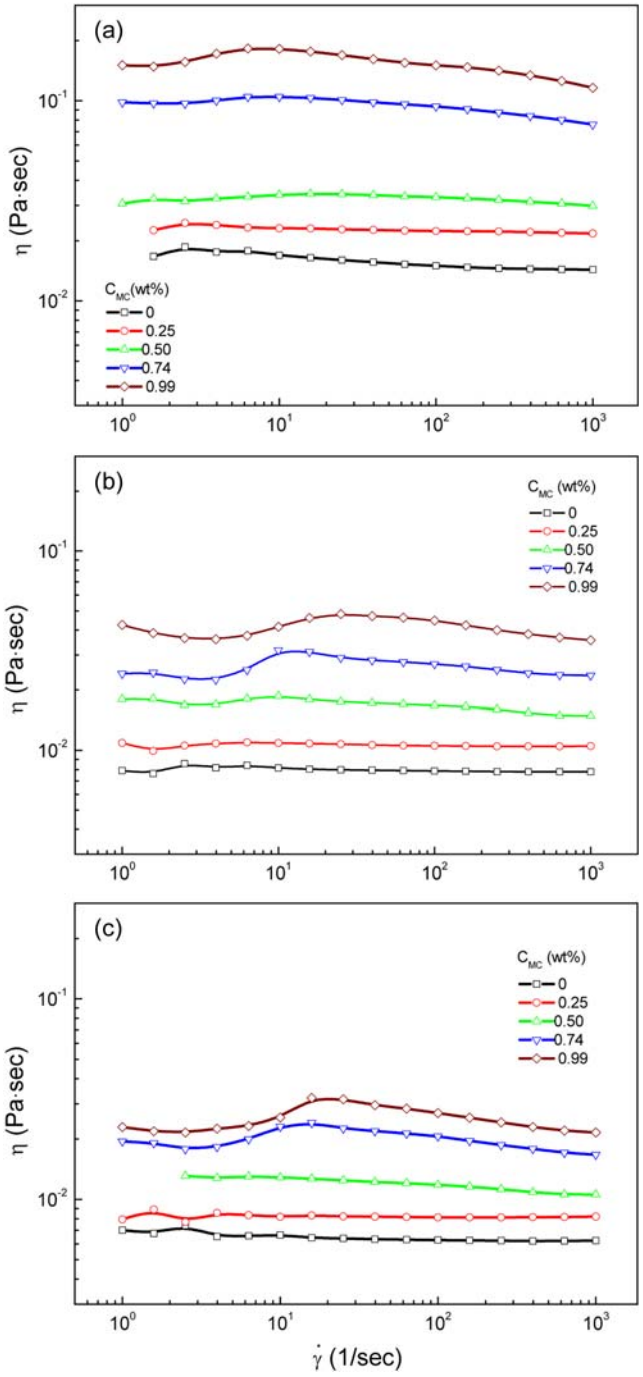

Fig. 1. Influence of MC concentration (C_{MC}) on apparent viscosity (η) as a function of shear strain rate ($\dot{\gamma}$) for the 10 wt% gliadin solutions at 15 (a), 35 (b), and 45°C (c).

Apparent viscosity (η) at $\dot{\gamma}$=100/sec as a function of reciprocal temperature $1/T$ for the solutions with different C_{MC} was shown in Fig. 2. η was linear dependent on reciprocal temperature $1/T$. Arrhenius law $\eta = A\exp(E_a/RT)$ was used to evaluate flow activation energy (E_a) at $\dot{\gamma}$ of 10, 100, and 1,000/sec, respectively. Here, A is a prefactor and R is gas constant. The E_a values at 3 strain rates are listed in Table 1 as a function of C_{MC}. The E_a value of the pure gliadin solution free of MC was determined as 21.4-24.3 kJ/mol, being in agreement with the reported values (23.5-27.3 kJ/mol) (31). The presence of MC caused an increase in E_a especially at $C_{MC} \geq 0.74$ wt%, which might be ascribed to the intermolecular hydrogen bonding interaction at high C_{MC}.

Morphology of films SEM micrographs of the blend films were shown in Fig. 3. The gliadin film (w_{MC}=0) showed tough fracture characteristic and the fracture surface contained abundant granular domains (Fig. 3a). The granular domains

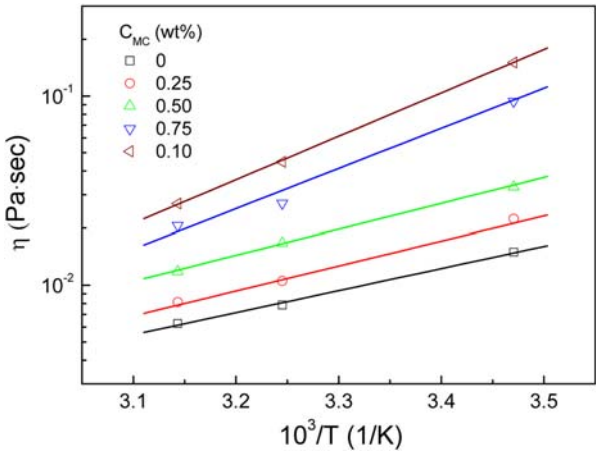

Fig. 2. Influence of MC concentration (C_{MC}) on apparent viscosity (η) as a function of reciprocal temperature $1/T$ for the 10 wt% gliadin solutions at strain rate of 100/sec.

Table 1. Influence of MC concentration C_{MC} on flow activation energy E_a for the 10 wt% gliadin solutions

C_{MC} (%)	E_a (kJ/mol)		
	$\dot{\gamma}$=10/sec	$\dot{\gamma}$=100/sec	$\dot{\gamma}$=1,000/sec
0	22.3±0.9	24.3±2.4	21.4±1.0
0.25	25.2±2.5	25.6±2.9	24.3±2.6
0.50	26.2±1.1	24.1±1.3	26.7±1.3
0.74	40.7±4.8	39.5±3.0	40.7±4.7
0.99	44.0±0.7	50.2±2.6	44.5±4.4

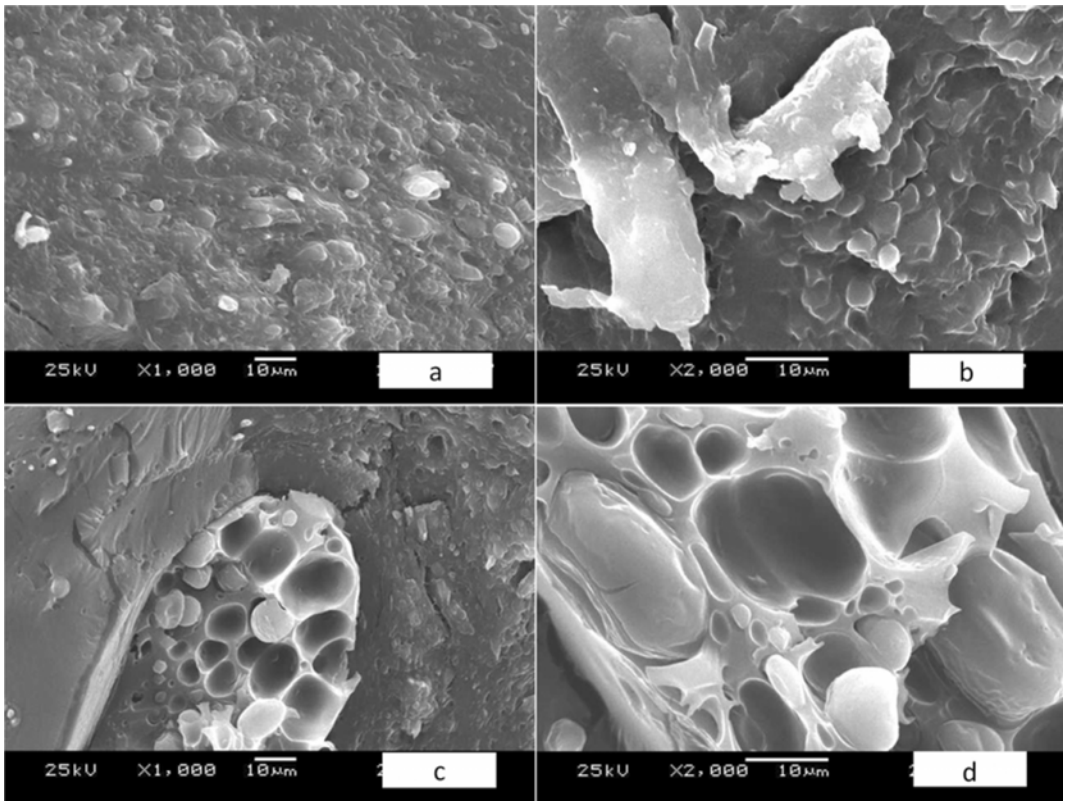

Fig. 3. SEM micrographs taken at the fracture surface of the blend films with MC weight percentage (w_{MC}) of 0 (a), 4.0 (b), 5.9 (c), and 7.7 wt% (d), respectively.

could also be identified in the gliadin phase in the blend film with w_{MC}=4.0 wt% (Fig. 3b). On the other hand, MC formed irregular aggregated structure with a size larger than 10 μm in the gliadin phase. In the blend film with w_{MC}=5.9 wt%, the gliadin phase formed smooth fracture surface (Fig. 3c). The size of the granular domains of the gliadin phase in the blend film was reduced considerably in comparison with the pure gliadin film. MC was present in the form of large ellipsoids in which small gliadin domains in the size of 10 μm were embedded. The morphology reveals that the mixture solutions underwent phase separation during the film drying process (27). The MC phase also exhibited brittle fracture characteristic, containing smooth concavities due to peeling off of the embedded gliadin domains. Figure 3d shows the morphology of the MC domain in the blend film with w_{MC}=7.7 wt%. The brittle fracture of the MC domain resulted in smooth surface.

FTIR spectra FTIR spectra of gliadin, MC and the blend films were shown in Fig. 4. The FTIR spectrum of the gliadin film exhibited a broad band in the 3,600-3,000 /cm range assigned to N-H stretching vibration (32). The absorption bands 1,750-1,580, 1,580-1,480, and 1,370-1,150/cm were related to amide I, amide II, and amide III, respectively (33). In the blend films, the positions of these bands did not vary with increasing C_{MC}. However, the increase in C_{MC} decreased the area intensity of these peaks, indicating that there might be interaction between MC and gliadins. The intermolecular interaction through hydrogen bonding might interfere with the gliadin structure at the gliadin-MC interface.

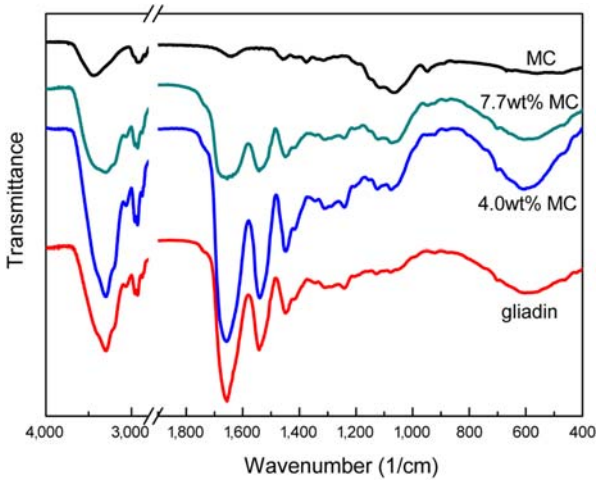

Fig. 4. FTIR spectra of gliadin and MC films and the blend films with w_{MC} of 4.0 and 7.7 wt%.

Mechanical properties Engineering stress-strain (σ-ε) relationship of the blend films at 50% RH was shown in Fig. 5. The gliadin film exhibited thermoplastic-like behavior with stress increasing rapidly at small strains but much slowly at ε>25%. Stress plateau and strain hardening appeared in succession at large strains. The blend films exhibited a marked yield stress at ε=15-25% followed by a stress drop. At larger strains after the stress drop, strain hardening was the main deformation mode in the blend film with w_{MC}=2.0 wt%, which was more significant than

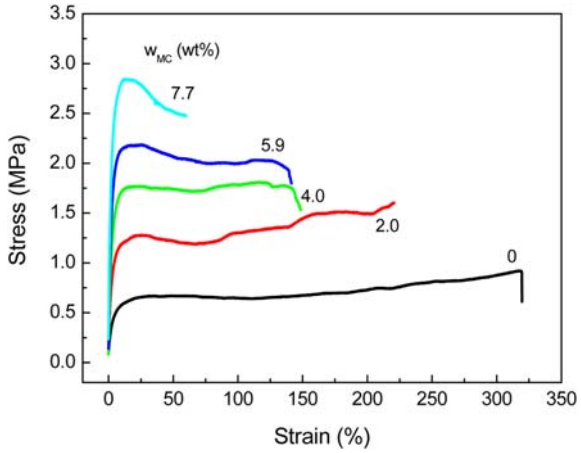

Fig. 5. Engineering stress-strain (σ-ε) relationship of the blend films at 50% RH.

Table 2. Influences of MC weight content w_{MC} on thickness (H), Young's modulus (E), tensile strength (σ_b), and strain at break (ε_b) for the blend films at 2 different relative humidies (RH)

w_{MC} (%)	H (μm)	E (MPa)	σ_b (MPa)	ε_b (%)
0	166±2[a1)]	18.2±2.1[e]	0.92±0.09[e]	319±21[a]
2.0	150±5[b]	55.9±1.2[d]	1.60±0.02[d]	219±15[b]
4.0	130±4[c]	68.8±0.7[c]	1.85±0.05[c]	141±2[c]
5.9	120±5[d]	102.8±6.0[b]	2.07±0.31[b]	130±4[d]
7.7	110±4[e]	150.6±9.9[a]	2.43±0.06[a]	60±2[e]

[1)]Means followed by different letters in the same column are significantly different (p<0.05).

in the gliadin film. The blend films with w_{MC}=2.4 and 4.0 wt% showed stress plateau up to ε=130%. On the other hand, the blend film with w_{MC}=7.7 wt% broke immediately after the stress drop.

Film thickness (H), Young's modulus (E), tensile strength (σ_b), and elongation at break (ε_b) as a function of w_{MC} for the blend films were shown Table 2. H decreased almost linearly with increasing w_{MC} with a correlation coefficient of –0.992 (p<0.05), from about 166 μm at w_{MC}=0 wt% to 110 μm at w_{MC}=7.7 wt%. Though η increased with increasing C_{MC}, the presence of MC seemed to facilitate the densification of the films due to the presence of intermolecular interaction, which leaded to the thickness reduction. E and σ_b increased while ε_b decreased with increasing w_{MC} (p<0.05). At w_{MC}=7.7 wt%, the E and σ_b values increased by 7.3 and 1.6 times, respectively, over the corresponding values at w_{MC}=0 wt%. The degeneration of extensibility was in accordance with the tough to brittle transition in fracture surface as shown in Fig. 3. MC consist of long straight chains that impart greater molecular order (34). The intermolecular interaction between MC and gliadins through hydrogen boning might be the main factor responsible for the improvement in E and σ_b in the blend films. The MC aggregation might be another reason for the reinforcement effect of MC to the gliadin films. The interaction between MC and gliadins restricted the molecular motion of gliadins, which gave rise to gradual reduction in ε_b with increasing w_{MC}. The blend films were

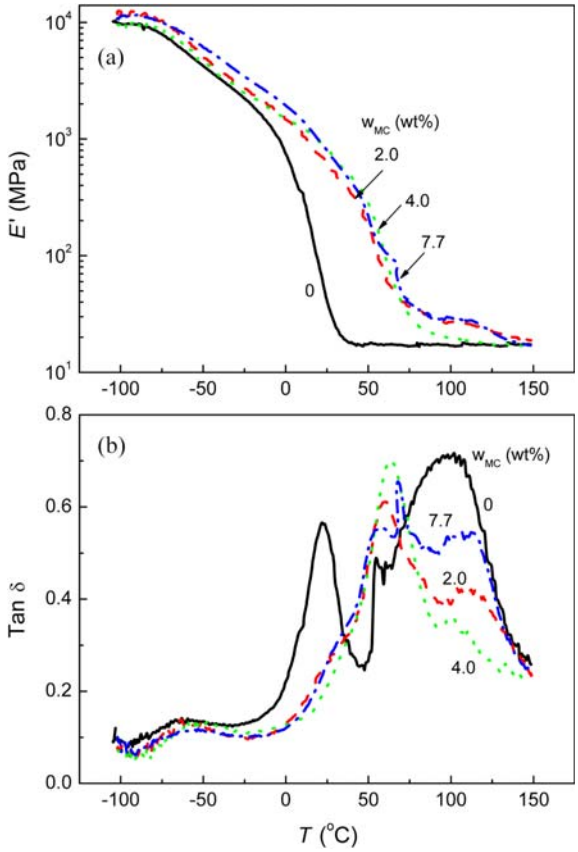

Fig. 6. Effects of MC content on storage modulus E' (a) and loss factor tan δ (b) for blend films.

weaker but more ductile than the MC films plasticized with 18 wt% polyethylene glycol (σ_b=25-33 MPa, ε_b=17-32%) (35).

Dynamical mechanical behavior Storage modulus (E') and loss factor (tan δ) at frequency of 1 Hz as a function of temperature T were shown in Fig. 6. The films traversed the glassy, the wide glass-to-rubber transition and the rubbery plateau regions in sequence with increasing T. E' decreased more than 2 orders of magnitude in the glassy transition region and the rapid E' decay of the blend film was shifted considerably to high temperatures in comparison with the gliadin film.

The gliadin film exhibited 3 tan δ peaks. A tiny peak at –62.8°C was related to the glass transition temperature (T_g) of the glycerol-rich domain (36), which was higher than T_g of pure glycerol at –93°C (37). The strong, sharp peak at 21.7°C corresponding to the sharp E' decay was related to T_g of the gliadin-rich domain, which was much lower than T_g of unplasticized gliadins ranging from 134 to 145°C (38) due to the plasticization of glycerol. The T_g of the gliadin-rich domain close to temperature of tensile test was responsible for the thermoplastic-like σ-ε curve with extensibility as high as 319%. The tan δ curve revealed another strong, broad tan δ peak appeared at T>50°C in the rubbery plateau region, which could be assigned to the crosslinking/aggregation reaction of gliadins through sulphydryl-disulfide interchange (39). The appearance of this high-temperature tan δ peak revealed that the

Table 3. Influences of MC weight content w_{MC} on moisture absorption (MA), water vapor permeability (WVP), and weight loss in water (WLW) for the blend films

w_{MC} (%)	MA at 70%RH (wt%)	WVP at 70%RH (10^{-11} g/m·sec·Pa)	WLW (wt%)	GSW[1)] (wt%)
0	20.2±0.2[a2)]	62.96±4.75[c]	34.8±3.8[e]	21.8[e]
2.0	19.9±0.2[a]	63.60±5.19[c]	40.4±3.6[d]	27.0[d]
4.0	19.7±0.1[a]	65.05±3.45[b,c]	45.3±2.9[c]	31.6[c]
5.9	19.7±0.2[a]	67.06±4.29[b]	49.8±3.1[b]	36.0[b]
7.7	19.5±0.2[a]	78.62±5.30[a]	51.6±4.4[a]	37.7[a]

[1)]Gliadin solubility in water.
[2)]Means followed by different letters in the same column are significantly different ($p<0.05$).

crosslinking reaction among gliadin molecules was not complete during the film formation at 50°C for 3 days. The thermal denaturation of gliadins from 58°C (40) could well account for the this high-temperature tan δ peak. In the rubbery plateau region, E' remained almost unvaried due to the thermally agitated softening balancing the crosslinking reaction.

In the blend films, T_g of the glycerol-rich domain increased slightly with increasing w_{MC} while T_g of the gliadin-rich domain was 36-41°C higher than that of the gliadin film. The elevated T_g of the gliadin-rich domain was involved in the occurrence of phase separation and the distribution of glycerol in the gliadin matrix and the MC disperse phase. It seemed that glycerol plasticizer was not dispersed homogeneously in the 2 components in the blend films. Increasing w_{MC} leaded to a reduction in degree of plasticization to the continuous gliadin matrix in the case of constant glycerol/gliadin ratio in the film. The large increase in T_g of the gliadin-rich domain was responsible for the appearance of yielding on the σ-ε curve (Fig. 5), the great reduction of ε_b of the blend film with respect to w_{MC} (Table 2), as well as the brittle fractures of the MC aggregates and the gliadin matrix at $w_{MC} \geq 5.9$ wt% (Fig. 3). The presence of MC hardly influenced the gliadin crosslinking/aggregation reaction as seen from the tan δ peak at around 100-112°C.

Water resistance Influence of w_{MC} on MA, WVP, and WLW of the blend films was shown in Table 3. MA did not vary ($p>0.05$) while WVP increased slightly with increasing w_{MC} ($p<0.05$). MC exhibited a higher water vapor transfer rate than wheat proteins (41), resulting in the increase of WVP with respect to w_{MC}. Similarly, WVP of whey protein/pullulan film increased with increasing pullulan/protein ratio from 0.1 to 1 (42). At given RH, WVP of the films was strongly related to the film forming condition and the plasticizer content. The WVP values of the blend films at 70% RH was comparable with the value 62×10^{-11} g/m·sec·Pa of wheat gluten film (28.6 wt% glycerol) at a relative higher RH (85%) (24) but was higher than the value $2\text{-}6\times10^{-11}$ g/m·sec·Pa of crosslinked gliadin and glutenin films (25-33 wt% glycerol) at lower RH (50-54%) (9,43,44). The WVP value of the blend films at 70% RH was considerably higher than the values of the unplasticized MC film ($2.3\text{-}10.9\times10^{-11}$ g/m·sec·Pa at 52% RH) (35) as well as MC film plasticized with 18 wt% polyethylene glycol ($7.0\text{-}11.6\times10^{-11}$ g/m·sec·Pa at 52% RH) (35) or 25 wt% glycerol (24.5×10^{-11} g/m·sec·Pa at 85% RH) (24).

All the films maintained their integrity in water because of the formation of intermolecular crosslinks between gliadins during film formation at 50°C. WLW increased significantly with increasing w_{MC} ($p<0.05$) because the MC component could be extracted completely in water (45). Gliadin solubility in water (GSW), defined as soluble gliadin fraction by the total gliadin fraction in the film, was estimated taking the glycerol and MC contents into consideration. The values of GSW are listed in Table 3 as a function of w_{MC}. GSW increased from 21.8 wt% in the gliadin film to 37.0 wt% in the blend film with w_{MC}=7.7 wt%, revealing that the presence of MC hindered the gliadin crosslinking reaction during film formation. Nevertheless, treatment of the film-forming solution using active chemical reagents is convenient to introduce chemical links between gliadin and MC, which should provide a straightforward way to make water resistant films and will be investigated later.

In conclusions, the presence of MC below 0.99 wt% improved viscosity and flow activation energy of the 10 wt% gliadin solution significantly. The gliadin/MC blend solutions were cast into blend films successfully. Morphological investigation showed that the MC component aggregates in the gliadin matrix. FTIR analysis evidenced the lack of intermolecular interaction between gliadin and MC. The blend films exhibited higher E and σ_b and lower ε_b in comparison with the gliadin film ($p<0.05$). The variation in mechanical performance was in agreement with the observation of the brittle fracture morphology of the MC component and the increase in T_g of the gliadin phase. Increasing MC content caused a slight increase in WVP ($p<0.05$). MC might hinder the gliadin crosslinking reaction during film formation so that GSW increased with increasing MC content.

Acknowledgments

This work was supported by the National Natural Science Foundation of China (50773068) and Natural Science Foundation of Zhejiang Province (Y407011).

References

1. Chabba S, Matthews GF, Netravali AN. 'Green' composites using cross-linked soy flour and flax yarns. Green Chem. 7: 576-581 (2005)
2. Gennadios A, Weller CL, Testin RF. Temperature effect on oxygen permeability of edible protein-based films. J. Food Sci. 58: 212-214, 219 (1993)
3. Fido RJ, Bekes F, Gras PW, Tatham AS. Effects of α-, β-, γ-, and ω-gliadins on the dough mixing properties of wheat flour. J. Cereal Sci. 26: 271-277 (1997)
4. Wieser H. Chemistry of gluten proteins. Food Microbiol. 24: 115-119 (2007)
5. Hernandez-Munoz P, Villalobos R, Chiralt A. Effect of thermal treatments on functional properties of edible films made from wheat gluten fractions. Food Hydrocolloid 18: 647-654 (2004)
6. Herald TJ, Gnanasambandam R, McGuire BH, Hachmeister KA. Degradable wheat gluten films: Preparation, properties, and applications. J. Food Sci. 60: 1147-1156 (1995)
7. Gao C, Stading M, Wellner N, Parker ML, Noel TR, Mills ENC,

Belton PS. Plasticization of a protein-based film by glycerol: A spectroscopic, mechanical, and thermal study. J. Agr. Food Chem. 54: 4611-4616 (2006)
8. Sanchez AC, Popineau Y, Mangavel C, Larre C, Gueguen J. Effect of different plasticizers on the mechanical and surface properties of wheat gliadin films. J. Agr. Food Chem. 46: 4539-4544 (1998)
9. Hernandez-Munoz P, Kanavouras A, Ng PKW, Gavara R. Development and characterization of biodegradable films made from wheat gluten protein fractions. J. Agr. Food Chem. 51: 7647-7654 (2003)
10. John J, Bhattacharya M. Properties of reactively blended soy protein and modified polyesters. Polym. Int. 48: 1165-1172 (1999)
11. Hernandez-Munoz P, Kanavouras A, Lagaron JM, Gavara R. Development and characterization of films based on chemically cross-linked gliadins. J. Agr. Food Chem. 53: 8216-8223 (2005)
12. Hernandez-Munoz P, Kanavouras A, Villalobos R, Chiralt A. Characterization of biodegradable films obtained from cysteine-mediated polymerized gliadins. J. Agr. Food Chem. 52: 7897-7904 (2004)
13. Debeaufort F, Voilley A. Methylcellulose-based edible films and coatings. 2. Mechanical and thermal properties as a function of plasticizer content. J. Agr. Food Chem. 45: 685-689 (1997)
14. Donhowe IG, Fennema O. The effects of plasticizers on cristallinity, permeability, and mechanical properties of methylcellulose films. J. Food Process. Pres. 17: 247-257 (1993)
15. Park HJ, Weller CL, Vergano PJ, Testin RF. Permeability and mechanical-properties of cellulose-based edible films. J. Food Sci. 58: 1361-1364 (1993)
16. Chinnan MS, Park HJ. Effect of plasticizer level and temperature on water vapor transmission of cellulose-based edible films. J. Food Process Eng. 18: 417-429 (1995)
17. Kamper SL, Fennema O. Water-vapor permeability of edible bilayer films. J. Food Sci. 49: 1478-1481 (1984)
18. Koelsch CM, Labuza TP. Functional, physical, and morphological properties of methylcellulose and fatty acid-based edible barriers. LWT-Food Sci. Technol. 25: 404-411 (1992)
19. Koelsch C, Labuza T. Functional, physical, and morphological properties of methyl cellulose and fatty acid-based edible barriers. LWT-Food Sci. Technol. 25: 404-411 (1992)
20. Kester JJ, Fennema O. An edible film of lipids and cellulose ethers-barrier properties to moisture vapor transmission and structural evaluation. J. Food Sci. 54: 1383-1389 (1989)
21. Erdohan ZO, Turhan KN. Barrier and mechanical properties of methyicellulose-whey protein films. Packag. Technol. Sci. 18: 295-302 (2005)
22. Turhan KN, Sancak ZOE, Ayana B, Erdogdu F. Optimization of glycerol effect on the mechanical properties and water vapor permeability of whey protein-methylcellulose films. J. Food Process Eng. 30: 485-500 (2007)
23. Coughlan K, Shaw NB, Kerry JF, Kerry JP. Combined effects of proteins and polysaccharides on physical properties of whey protein concentrate-based edible films. J. Food Sci. 69: E271-E275 (2004)
24. Park HJ, Chinnan MS. Gas and water vapour barrier properties of edible films from protein and cellulosic materials. J. Food Eng. 25: 497-507 (1995)
25. Park SK, Bae DH. Antimicrobial properties of wheat gluten-chitosan composite film in intermediate-moisture food systems. Food Sci. Biotechnol. 15: 133-137 (2006)
26. Fakhouri FM, Tanada-Palmu PS, Grosso CRF. Characterization of composite biofilms of wheat gluten and cellulose acetate phthalate. Braz. J. Chem. Eng. 21: 261-264 (2004)
27. Turgeon SL, Beaulieu M, Schmitt C, Sanchez C. Protein-polysaccharide interactions: Phase-ordering kinetics, thermodynamic, and structural aspects. Curr. Opin. Colloid In. 8: 401-414 (2003)
28. Turgeon SL, Beaulieu M. Improvement and modification of whey protein gel texture using polysaccharides. Food Hydrocolloid 15: 583-591 (2001)
29. ASTM. Standard test methods for water vapour transmission of materials. E96-80. In: ASTM Annual Book of American Standard Testing Methods. American Standard Testing Materials, Philadelphia, PA, USA (1983)
30. Letendre M, D'Aprano G, Lacroix M, Salmieri S, St-Gelais D. Physicochemical properties and bacterial resistance of biodegradable milk protein films containing agar and pectin. J. Agr. Food Chem. 50: 6017-6022 (2002)
31. Sun S, Song Y, Zheng Q. Rheological behavior of wheat gliadins in 50%(v/v) aqueous propanol. J. Food Eng. 90: 207-211 (2009)
32. Moharram MA, Abd-El-Nour KN. Infrared spectra and dielectric properties of thermally treated soybean proteins. Polym. Degrad. Stabil. 45: 429-434 (1994)
33. Robertson GH, Gregorski KS, Cao TK. Changes in secondary protein structures during mixing development of high absorption (90%) flour and water mixtures. Cereal Chem. 83: 136-142 (2006)
34. Banerjee R, Chen H. Functional properties of edible films using whey protein concentrate. J. Dairy Sci. 78: 1673-1683 (1995)
35. Turhan KN, Sahbaz F. Water vapor permeability, tensile properties, and solubility of methylcellulose-based edible films. J. Food Eng. 61: 459-466 (2004)
36. Sun S, Song Y, Zheng Q. Morphologies and properties of thermo-molded biodegradable plastics based on glycerol-plasticized wheat gluten. Food Hydrocolloid 21: 1005-1013 (2007)
37. Cherian G, Gennadios A, Weller C, Chinachoti P. Themomechanical behavior of wheat gluten films: Effect of sucrose, glycerin, and sorbitol. Cereal Chem. 72: 1-6 (1995)
38. Noel TR, Parker R, Ring SR, Tatham AS. The glass-transition behaviour of wheat gluten proteins. Int. J. Biol. Macromol. 17: 81-85 (1995)
39. Ahmed J, Ramaswamy HS, Raghavan VGS. Dynamic viscoelastic, calorimetric, and dielectric characteristics of wheat protein isolates. J. Cereal Sci. 47: 417-428 (2008)
40. Leon A, Rosell CM, de Barber CB. A differential scanning calorimetry study of wheat proteins. Eur. Food Res. Technol. 217: 13-16 (2003)
41. Debeaufort F, Voilley A. Aroma compound and water vapor permeability of edible films and polymeric packagings. J. Agr. Food Chem. 42: 2071-2075 (1994)
42. Gounga ME, Xu SY, Wang Z. Whey protein isolate-based edible films as affected by protein concentration, glycerol ratio, and pullulan addition in film formation. J. Food Eng. 83: 521-530 (2007)
43. Hernandez-Munoz P, Lopez-Rubio A, Del-Valle V, Almenar E, Gavara R. Mechanical and water barrier properties of glutenin films influenced by storage time. J. Agr. Food Chem. 52: 79-83 (2004)
44. Hernandez-Munoz P, Villalobos R, Chiralt A. Effect of cross-linking using aldehydes on properties of glutenin-rich films. Food Hydrocolloid 18: 403-411 (2004)
45. Song Y, Zheng Q. Structure and properties of methylcellulose microfiber reinforced wheat gluten based green composites. Ind. Crop. Prod. 29: 446-454 (2009)